Determination of arsenic and antimony in seawater by voltammetric and chronopotentiometric stripping using a vibrated gold microwire electrode

ARTICLE *in* ANALYTICA CHIMICA ACTA · OCTOBER 2012

Impact Factor: 4.51 · DOI: 10.1016/j.aca.2012.08.013 · Source: PubMed

Analytica Chimica Acta 746 (2012) 53–62

Contents lists available at SciVerse ScienceDirect

Analytica Chimica Acta

journal homepage: www.elsevier.com/locate/aca

Determination of arsenic and antimony in seawater by voltammetric and chronopotentiometric stripping using a vibrated gold microwire electrode

Pascal Salaün[a,*], Kristopher B. Gibbon-Walsh[a,1], Georgina M.S. Alves[b], Helena M.V.M. Soares[b], Constant M.G. van den Berg[a]

[a] School of Environmental Sciences, University of Liverpool, 4 Brownlow Street, L69 3GP Liverpool, United Kingdom
[b] REQUIMTE, Departamento de Engenharia Química, Faculdade de Engenharia, Universidade do Porto, Rua. Dr. Roberto Frias, 4200-465 Porto, Portugal

HIGHLIGHTS

- Inorganic speciation of arsenic and antimony in seawater at a gold electrode.
- Sensitive methods both in relatively low acidic and in neutral conditions of pH.
- New experimental approaches to decrease detection limits and avoid interferences.
- As^{III} remains adsorbed on the gold surface after stripping during a short time.
- On-board analysis of As(III) at sub nanomolar levels.

GRAPHICAL ABSTRACT

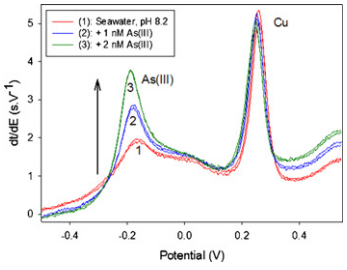

ARTICLE INFO

Article history:
Received 15 June 2012
Received in revised form 30 July 2012
Accepted 8 August 2012
Available online 19 August 2012

Keywords:
Metalloids
Speciation
Seawater
Stripping
Vibrated gold microwire electrode
Monitoring

ABSTRACT

The oxidation potentials of As^0/As^{III} and Sb^0/Sb^{III} on the gold electrode are very close to each other due to their similar chemistry. Arsenic concentration in seawater is low (10–20 nM), Sb occurring at ~0.1 time that of As. Methods are shown here for the electroanalytical speciation of inorganic arsenic and inorganic antimony in seawater using a solid gold microwire electrode. Anodic stripping voltammetry (ASV) and chronopotentiometry (ASC) are used at pH ≤ 2 and pH 8, using a vibrating gold microwire electrode. Under vibrations, the diffusion layer size at a 5 μm diameter wire is 0.7 μm. The detection limits for the As^{III} and Sb^{III} are below 0.1 nM using 2 min and 10 min deposition times respectively. As^{III} and Sb^{III} can be determined in acidic conditions (after addition of hydrazine) or at neutral pH. In the latter case, oxidation of As^0 to As^{III} was found to proceed through a transient As^{III} species. Adsorption of this species on the gold electrode at potentials where Sb^{III} diffused away is used for selective deposition of As^{III}. Addition of EDTA removes the interfering effect of manganese when analysing As^{III}. Imposition of a desorption step for Sb^{III} analysis is required. Total inorganic arsenic (iAs = $As^V + As^{III}$) can be determined without interference from Sb nor mono-methyl arsenious acid (MMA) at 1.6 < pH < 2 using $E_{dep} = -1$ V. Total inorganic antimony (iSb = $Sb^V + Sb^{III}$) is determined at pH 1 using $E_{dep} = -1.8$ V without interference by As.

The methods were tested in samples from the Irish Sea (Liverpool Bay). As^{III} was determined on-board ship immediately after sampling. As^{III} concentrations were found to range from 0.44 to 1.56 nM and were higher near the coast. Sb^{III} was below the detection limit (<0.1 nM Sb^{III}), iAs was comprised between 8 and 25 nM while iSb varied from 0.5 to 1.7 nM.

* Corresponding author.
E-mail addresses: salaun@liverpool.ac.uk, pascal.salaun@liv.ac.uk (P. Salaün).
[1] Present address: RMCO-PROTEE Laboratory, University of Toulon-Var, Boite postale 132, 83957 La Garde, France.

0003-2670/$ – see front matter.
http://dx.doi.org/10.1016/j.aca.2012.08.013

1. Introduction

Arsenic and antimony occur in seawater at concentrations of 10–20 nM As [1,2] and 0.4–1.6 nM Sb [3]. The inorganic oxidised (+5) species (arsenate and antimonate) are predominant in oxic waters, the reduced (+3) species occurring at much lower levels due to biotic and abiotic reduction processes coupled with slow oxidation kinetics. Methylated species also occur, including monomethyl arsenic acid (MMA), dimethyl arsenic acid (DMA), monomethyl stibonic acid (MMSb) and other organic species (arsenosugars) [4,5]. In ocean waters the speciation of arsenic is largely defined by phytoplankton activity [6]. As a phosphate analogue, competitive uptake with arsenate occurs causing a nutrient-like oceanic depth profile [7,8]. Dissolved arsenite, MMA and DMA are mostly restricted to the upper water column [8] as they are excreted by phytoplankton in response to arsenate uptake [9,10]. Antimony shows a mildly scavenged behaviour in ocean waters with either conservative behaviour or slightly decreasing levels with depth, probably due to anthropogenic atmospheric inputs [9]. Sb^{III} and MMSb are found in surface waters [9] at low levels (~0.05 nM).

The speciation of arsenic and antimony in seawater is usually determined by hydride generation (HG) methods [11] coupled to atomic absorption spectroscopy (AAS) [12–14] or atomic fluorescence spectroscopy (AFS) [15]. Other methods are based on dispersive liquid–liquid extraction [16,17], solid phase extraction [18], total reflection X-ray fluorescence spectrometry (TXRF) [19] or co-precipitation [20,21].

Although bulky, these techniques were used on-board for As and Sb speciation. HG followed by cryogenic trapping, gas chromatography and photo-ionization detection [6] with detection limits of ~1 pM for inorganic species, ~5 pM for methylated species were used by Cutter et al. in open oceans [6,9]. HG-AFS for As speciation were used [22,23].

Electroanalytical methods can be an alternative for the inorganic speciation of these species. They present the advantage to be portable and relatively inexpensive with low detection limit for a number of trace elements. They can be used on-board which prevents problems related to storage, especially regarding the trivalent species [19,24]. Though electroanalytical methods exist for As and/or Sb in aqueous media, few have focused on the speciation in seawater. Detection of natural levels of arsenic has mostly been achieved on gold electrodes [25–31] either by anodic stripping voltammetry (ASV) or anodic stripping chronopotentiometry (ASC) but also on mercury electrodes [32,33] by cathodic stripping voltammetry (CSV) and on bismuth film electrode [34,35]. Determination of inorganic species of Sb in sea water has mostly been achieved at Hg electrodes by ASV [36–39] and CSV [40,41] with comparatively little work on seawater using gold [42–44] or bismuth electrodes [45]. Speciation is complicated by several problems related to contamination and changes due to sample modification: (1) the perceived electro-inactivity of the pentavalent species (especially Sb^{V}) which need to be chemically reduced prior to their determination. Chemical reducing agents such as L-cysteine [27,42], sulphur dioxide [38,39] or potassium iodide [28] are commonly used; (2) the use of strong acidic conditions to increase the sensitivity [36]; and (3) the use of reducing agents such as ascorbic acid [36] and hydrazine [27–29] to avoid oxidation of the trivalent species. In addition, the sensor surface must be robust with a constant response for a significant amount of time.

The detection of As and Sb trivalent species in seawater is challenging due to low concentrations. As^{III} can be detected at low levels by voltammetry using gold electrodes [27,29–31,46,47] while natural levels of Sb^{III} (0.1 nM and less) are at, or below, the limit of detection for mercury electrodes (0.1 nM Sb^{III}) in acidic conditions even using a 10-min plating time [36,39,48]. Recent work has shown that very good sensitivity is obtained for Sb^{V} when the deposition potential is very negative, well inside the hydrogen wave [44].

In this report, we present procedures for the speciation of inorganic antimony and inorganic arsenic, making use of a vibrating gold microwire electrode in conjunction with selective deposition from inside the hydrogen wave, selective re-oxidation and judicious conditioning potential steps where possible. Vibrations have been shown to enhance mass transport [49], strongly improve reproducibility [50] and lower detection limits. They also allow the use of very negative deposition potentials in acidic conditions by removing hydrogen from the electrode surface, property highly beneficial for Sb detection [44]. The work achieves determination of inorganic As and Sb without the need for chemical reducing agents in mild acidic conditions (pH 1–2). As^{III} and Sb^{III} are detected selectively either at natural pH or in weakly acidic conditions (pH ~2–3) with detection limits reaching tens of pM which should allow detection of these species in freshly collected open ocean waters. The methods were tested on coastal waters either on-board ship or in the laboratory.

2. Experimental

2.1. Chemicals

Water used to prepare reagents and preliminary working solutions was 18 MΩ cm^{-1} purified using a Millipore-Elix system. HCl was purified by sub-boiling distillation on a quartz condenser. Standard Sb^{V} and Sb^{III} solutions were prepared by dilution with water of 1000 ppm standard solutions from Aldrich and BDH respectively. As^{V} and As^{III} were obtained after dissolving $HAsO_2$ and As_2O_3 salts in water and in 0.1 M NaOH respectively before acidification to pH 2 using HCl. Standard solutions were kept at room temperature. Sb^{III} and As^{III} standard solutions were wrapped in aluminium foil to avoid potential photo-oxidation and were used for a maximum of 2 months. Hydrazine chloride (N_2H_4-2HCl, puriss p.a. grade 99.99%, Aldrich), hydrazine sulphate (N_2H_4-H_2SO_4 – 99.999% trace metal basis, Aldrich), H_2SO_4 (BDH Chemicals Ltd, AnalaR grade, UK), EDTA (Fluka), $K_3Fe(CN)_6$, KCl (AnalaR grade, BDH, UK) and $NaNO_3$ (AnalaR grade, BDH) were used. Monosodium acid methane arsonate sesquihydrate (MMA) and sodium cacodylate trihydrate (DMA) were from Greyhound Chromatography and Allied Chemicals (Birkinhead, UK) and Sigma (UK) respectively. Method optimisations were done in filtered seawater (0.2 μm using a Sartobran® 300 filtration cartridge) collected in Liverpool Bay.

2.2. Equipment, electrode fabrication

Voltammetric experiments were made using a μAutolabIII potentiostat (EcoChemie, now Metrohm AG, Switzerland) computer controlled using GPES software (version 4.9). A three electrode cell containing the gold microwire working electrode (WE), an iridium counter electrode (CE) (150 μm diameter, ~3 mm length), and a double-junction, Ag/AgCl/KCl (3 M)//$NaNO_3$ (0.1 M), reference electrode were placed in a voltammetric cell (Teflon), which was placed in a Faraday cage (Windsor Scientific, UK). For some experiments with dilute model solutions the salt bridge was filled with 0.1 M $NaNO_3$. Gold microwires (Purity: 99.99%, temper: hard) of 5, 10 and 25 μm diameter (Goodfellow, UK) were used for the electrodes. A vibrator rotor was attached to the microwire WE [49]. The vibrator, used in place of a standard magnetic stirrer, was powered by an IME663 (EcoChemie) controlled by GPES software. The vibrated gold microwire electrodes were prepared as described previously [30] and stored in air or Milli-Q water.

The surface of the electrode was cleaned electrochemically in 0.5 M H_2SO_4 by hydrogen generation at −2.5 V for 30 s prior to use

twice daily. The reduction peak of the oxide monolayer obtained in 0.5 M H_2SO_4 was used to monitor the surface area [51].

2.3. Determination of As^V, Sb^V, As^{III} and Sb^{III}

As^{III} and Sb^{III} were measured by ASC at neutral pH or in acidic conditions with the addition of hydrazine. Sb^V was determined by differential pulse ASV (100 ms interval time, 2–6 ms modulation time, 25 mV amplitude, 4–6 mV step) in seawater acidified to pH ~ 1 by using a very negative deposition potential (−1.8 V). As^V was measured either by square wave ASV (50 mV amplitude, 50 Hz and 8 mV step) or ASC in acidified seawater (pH < 2) using a deposition potential of −1 V. In each case, a background scan was recorded in similar conditions as the main analytical scan but with only a short deposition time (1–3 s). The background corrected scan (analytical–background) was always used for analysis. In ASV, the peak derivative (measured automatically by the GPES software) was used for quantification while the peak area (linear baseline, manually selected) was used in ASC. All measurements were calibrated by standard additions to the sample with a minimum of three additions and three measurements per additions. The sample concentrations and the analytical standard deviation were calculated using the LINEST function (Excel) including all scans obtained within the linear range.

pH experiment was achieved in deoxygenated buffered solution composed of 10 mM Na_2SO_4, 30 mM Na_2CO_3 (pK_a: 6.4, 10.4), 10 mM H_3BO_3 (pK_a: 9.2) and 2 mM Na_2HPO_4 (pK_a: 2.15, 7.2, 12.4). The pH was first adjusted to pH ~ 12 with NaOH and lowered by addition of H_2SO_4 (0.001–0.1 M).

2.4. Field testing of the new methods for As^{III} and Sb^{III}

10 samples were collected at 7 m depth during a cruise with the RV Prince Madog (April 2011) in Liverpool Bay (Irish Sea). Samples were collected using a metal-free Niskin bottle filtered on-line (0.2 μm – Sartobran300) into acid washed LDPE Nalgene bottles (Fisher – UK) and analysed within 2 h on-board ship. In additions, samples collected in June 2009 and September 2010 were acidified on-board to pH 2 and analysed in laboratory conditions within 6 months for total inorganic arsenic (iAs) and total inorganic antimony (iSb).

3. Results and discussion

Electrode characteristics: diffusion layer thickness

The electrode length (L) was determined in the same manner as previously described [51]. The diffusion layer thickness (Eq. (1)) under vibrated conditions was calculated from the diffusion limited current (I_{SS}) obtained for the reduction of 10 mM $K_3Fe(CN)_6$ in 0.5 M KCl.

$$\delta = \frac{nF\pi \varnothing LDC_{bulk}}{I_{SS}} \quad (1)$$

with δ = the diffusion layer of $Fe(CN)_6^{3-}$, n = the number of exchanged electrons (1), F = the faraday constant (96,500 C mol^{-1}), $\varnothing$ = the diameter (cm), D = the diffusion coefficient of $Fe(CN)_6^{3-}$ in 0.5 M KCl (7.17×10^{-6} cm^2 s^{-1}) and C_{bulk} is $Fe(CN)_6^{3-}$ bulk concentration (mol cm^{-3}). Roughness coefficients at the 5, 10 and 25 μm diameter wires were determined by dividing the real surface area (given by the reduction charge of the gold-oxide monolayer obtained by cyclic voltammetry in 0.5 M H_2SO_4) by the geometric area. Diffusion limited currents obtained in quiescent solution, stirred and vibrated conditions were compared (Fig. 1A). Under vibrated conditions, the diffusion current at the 5 μm wire electrodes was 2.6 times higher and had a much smaller standard deviation (RSD = 0.42%) than that with a magnetic stirrer (RSD = 14%), in agreement with previous result at a vibrated Bi disc electrode [50]. Diffusion layer thicknesses and roughness values are summarised in Table 1. They are remarkably small for such simple devices and ensure low detection limit in anodic stripping techniques. Using conventional, non-vibrated, electrodes, a diffusion layer thickness of 2 μm has been achieved using a high-speed rotating disk electrode (39,000 rpm) [52]. The higher roughness value at the 5 μm ⌀ electrode was confirmed by SEM imaging (Fig. 1B) which clearly shows longitudinal patterns of ~200 nm width which are produced when the gold is pulled at the right diameter (Fig. 1). The same patterns are less apparent on the 10 and 25 μm diameter wires due to their larger diameter. These low roughness values increase the faradaic/capacitive current ratio and thus also contribute to low detection limits.

Table 1
Diffusion layer and roughness values obtained at the vibrated microwire electrodes. N is the number of electrodes tested.

Diameter (μm)	Diffusion layer (μm)	Roughness	N
5	0.7 ± 0.1	1.5 ± 0.3	5
10	1.1 ± 0.1	1.2 ± 0.1	4
25	2.0 ± 0.2	1.2 ± 0.2	4

Electrode stability

The same electrode was calibrated daily for the detection of Sb^{III} over a period of 10 days by ASC. The sensitivity was 29.3 ± 1.8 ms nM^{-1} (n = 10), corresponding to a RSD of 6.1%. The wire electrodes can be used for periods of weeks with good reproducibility. Regular (daily to twice daily) cleaning by hydrogen

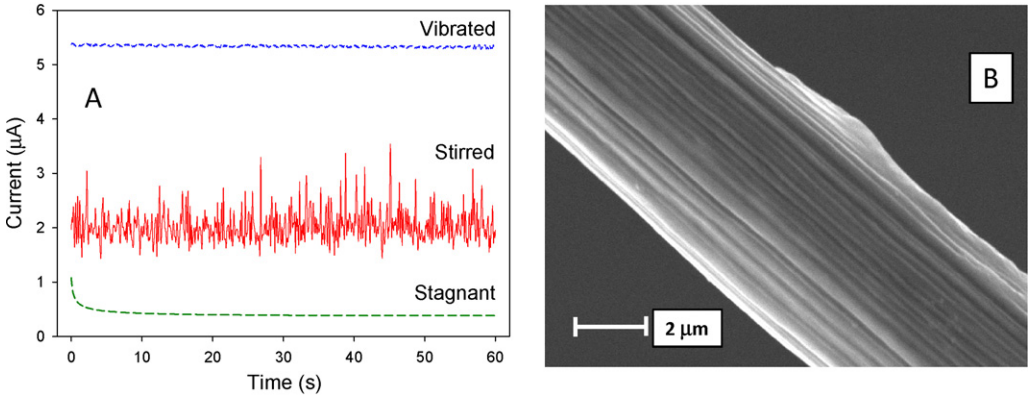

Fig. 1. (A) Chronoamperometric response of a 5 μm gold microwire electrode (length of ~360 μm) in 11 mM $K_3Fe(CN)_6$ under stagnant, stirred and vibrated conditions. (B) SEM picture of a 5 μm diameter gold wire.

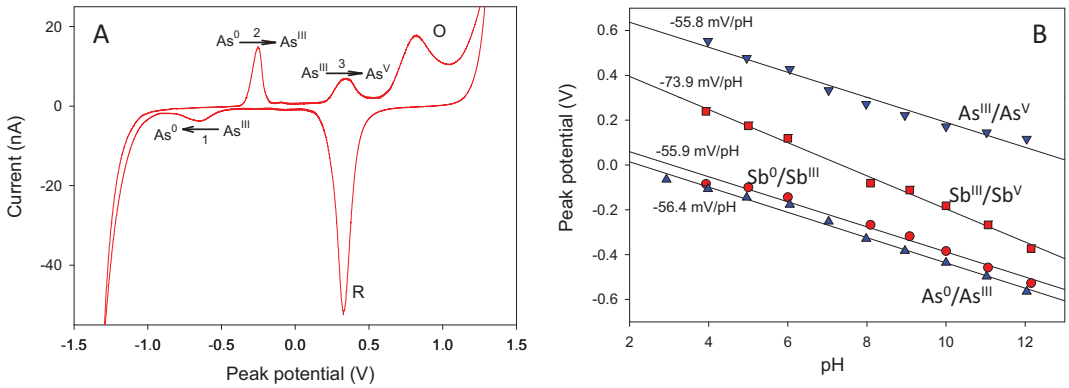

Fig. 2. (A) Cyclic voltammogram of 10 μM As^{III} at pH 7.02 (100 mV s^{-1}) – CV started at −0.2 V. 1, 2 and 3 represents chronological order. (B) Effect of pH on the peak potentials – solution: 10 mM Na_2SO_4 + 30 mM Na_2CO_3 + 10 mM H_3BO_3 + 2 mM Na_2HPO_4 + 10 mM Sb(III) or 2 mM As(III). pH adjusted with NaOH and H_2SO_4.

generation in 0.5 M H_2SO_4 at a negative potential (−2.5 V) and using a standby potential (0.55 V) between measurements were used to improve stability.

3.1. Determination of trivalent inorganic As^{III} and Sb^{III}: separation of As^{III} and Sb^{III}

In sea water, the peak potentials for As^{III} and Sb^{III} on the gold electrode are separated by ~40 mV [25] causing the peaks to overlap. Medium exchange with a stripping medium of 4 M HCl/4 M $CaCl_2$ [53] or strong alkaline conditions (0.1 M NaOH) [54] were successful in resolving the two peaks. The effect of pH on peak resolution was assessed by measuring the stripping peak potentials of As^0 and Sb^0 in the mixed buffer solution. A typical voltammogram obtained for 10 μM As^{III} is shown in Fig. 2A. Same behaviour was also observed for Sb^{III}. As^{III}/Sb^{III} is first reduced to As^0/Sb^0 during the cathodic scan of the CV, and oxidised to As^{III}/Sb^{III} (Eqs. (2)/(3)) and subsequently to As^V/Sb^V (Eqs. (4)/(5)) during the anodic scan, in agreement with previous study [55]. The peaks O and R (Fig. 2A) are due to the gold oxidation and reduction of the oxides respectively. The peak potentials were found to shift linearly with pH (Fig. 2B). These shifts were close to the expected values of −59 mV/pH for Eqs. 2, 3 and 4 (−56.4, −55.9 and −55.8 mV) while a significant discrepancy was observed for Sb^{III}/Sb^V (Eq. (5)) (experimental value of −73.9 mV/pH against an expected slope of −88 mV).

$$As^0 + 3H_2O \rightarrow AS(OH)_3{}^0 + 3H^+ + 3e^- \quad (2)$$

$$Sb^0 + 3H_2O \rightarrow Sb(OH)_3{}^0 + 3H^+ + 3e^- \quad (3)$$

$$AS(OH)_3{}^0 + H_2O \rightarrow OAS(OH)_3 + 2H^+ + 2e^- \quad (4)$$

$$Sb(OH)_3{}^0 + 3H_2O \rightarrow Sb(OH)_6{}^- + 3H^+ + 2e^- \quad (5)$$

$$AS(OH)_3{}^0 + 3H^+ + 3e^- \rightarrow AS^0 + 3H_2O \quad (6)$$

In un-buffered solutions, it was noticed that redox processes cause the pH at the surface of the electrode to be lower (Eqs. (2) and (4) – release of protons) or higher (Eq. (6) – consumption of protons) than in the bulk of the solution, resulting in inverted S-shape curves when plotting Ep vs pH (Fig. S1 in supplementary material), similar to previously reported results [25].

3.1.1. Effect of the deposition potential

The influence of the deposition potential on As^{III} and Sb^{III} peak intensity was assessed at natural pH and in acidified (pH 1) sea water (Fig. 3). Hydrazine was added to the solution to prevent chemical oxidation of As^{III}/Sb^{III} that could occur either through the reduction of iodate in acidic conditions (Eq. (7) known as Duschman reaction) followed by oxidation with tri-iodide (Eq. (8) known as Roebuck reaction) [36,56] or through oxidation with hypochloric acid formed at the auxiliary electrode [25]:

$$IO_3{}^- + 5I^- + 6H^+ \rightarrow 3I_2 + 3H_2O \quad (7)$$

$$AS(OH)_3{}^0 + I_3{}^- + H_2O \rightarrow H_3AsO_4 + 3I^- + 2H^+ \quad (8)$$

The presence of hydrazine was found to be very efficient in preventing the oxidation of As^{III} and Sb^{III}. Without hydrazine, 5 nM As^{III} was oxidised within seconds in acidified seawater (pH 1) due to the chlorine generated at the auxiliary electrode when a low deposition potential (−1.0 V) was used. In presence of 100 μM hydrazine, the peak intensity of 5 nM As^{III} decreased only by 25% after 30 min at −1.0 V. Separate experiments showed that the hydrazine did not reduce Sb^V or As^V so it could be added without causing interference.

The variation of the deposition potentials showed that Sb^{III} can be determined without interference from As^{III} by selecting relatively positive deposition potentials: using $E_{dep} \geq -0.5$ V and $E_{dep} \geq -0.2$ V at natural pH and in acidic conditions respectively (Fig. 3). At neutral pH, both As^{III} and Sb^{III} give a signal at potential below −0.5 V with similar intensity at sufficiently negative deposition potentials ($E \leq -1$ V). The section below presents optimised analytical procedures for the selective determination of As^{III} and Sb^{III} in de-oxygenated sea water at natural pH and without de-oxygenation in acidified sea-water.

3.2. Optimum conditions for Sb^{III} determination

3.2.1. At natural pH

As^{III} can interfere with the determination of Sb^{III} due to proximity of their peaks at any pH (Fig. 2) and due to higher concentration levels of As. There is only a narrow range (Fig. 3) of deposition potential (−0.4 V > E_{dep} > −0.5 V) that can be used to avoid the effect of As^{III}. However, if the stripping step was started from this positive deposition potential, the peak shape of Sb^{III} was very poor (Fig. 4A). This problem was resolved by applying a desorption step (consisting in the application of a negative potential (e.g. −1.2 V) for a short time (1–3 s) just before the stripping step), which much improved the peak shape of Sb^{III}, and also of Cu and Hg. It is known that this desorption potential minimises the amount of adsorbed anions and dissolved organic matter (DOM) [51,57] at the gold surface. A similar desorption step has been used for the detection of Cu with a Hg drop electrode [58]. This desorption step is required as UV-digestion cannot be used to remove the interfering effect of DOM as this caused the signal for Sb^{III} to disappear, probably through oxidation to Sb^V. The application of this desorption step is always recommended if the deposition potential is >~−1 V.

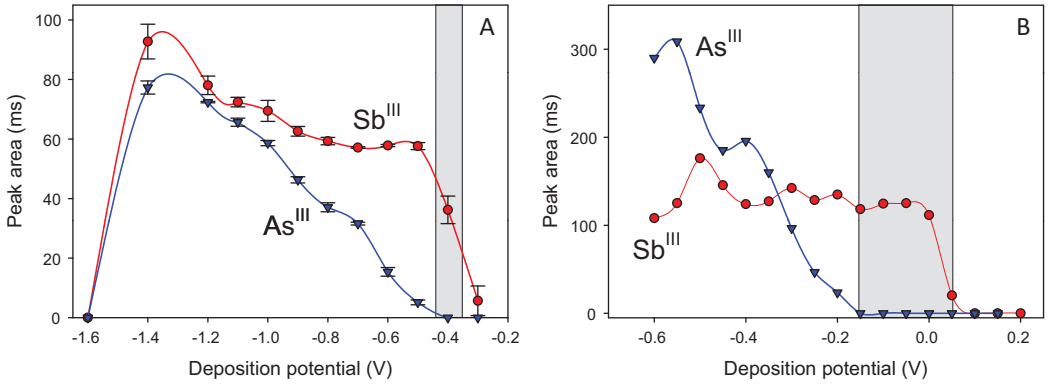

Fig. 3. ASC response for 10 nM As^{III} and 10 nM Sb^{III} as a function of deposition potential in purged seawater at pH ~8.4 (A) and oxygenated seawater at pH ~1 (B). Solution B contained 80 μM hydrazine. The electrodes used in A and B had different lengths. The grey areas indicate the regions where Sb^{III} determination is not affected by the presence of As^{III}.

Additions of Sb^{III} (Fig. 4A and Fig. S2) to sea-water caused the formation of two peaks at ~−200 mV and ~−40 mV whilst only one peak was expected for the Sb^0/Sb^{III} redox couple. The presence of the second peak suggests that after reoxidation of Sb^0 to Sb^{III}, some of the newly formed Sb^{III} remains adsorbed at the surface of the gold until it is further oxidised to Sb^V which diffuses away. The charge ratio between the two peaks was well below the 66% predicted by Eqs. (3) and (5) suggesting that, within the time scale of the experiment, not all the Sb^{III} produced after oxidation of Sb^0 is adsorbed at the gold surface but some has diffused away before further oxidation to Sb^V could occur.

The desorption step caused the Sb^{III} peak to become sharp and well resolved (Fig. 4A). A well defined diffusion limited signal occurs between −0.4 V and −1.2 V (Fig. 4B) when the desorption step is used, while this expected response is not observed without the desorption step. Its effect is most beneficial at positive deposition potentials (Fig. 4B) which is convenient as then Sb^{III} is deposited without As^{III}. The desorption step was always implemented for the determination of Sb^{III}. Some As^{III} is plated on the gold surface during this step but this effect is minimal because the desorption step is brief, and it is also applied in the background scan which means that its contribution is removed in the background corrected scan.

3.2.2. Acidic conditions

In acidic conditions (pH ≤ 3), the peak of Sb^{III} is positive of oxygen reduction making de-oxygenation unnecessary. At this pH, ASC was found to give better peak current/noise ratio than ASV. The desorption step at −1.2 V for 1 s improved the sensitivity at low pH, as at natural pH. Although the sensitivity for Sb^{III} (tested at 2 nM Sb) was similar in seawater acidified with 10 or 50 mM HCl, the analysis of sub nM levels was improved in 50 mM HCl as the baseline was flatter and the peak better resolved from that for Cu than when using 10 mM HCl. The deposition potential had to be ≥−0.18 V to avoid interference from 2 nM As^{III} (Fig. S3 shows the response for As^{III}, Sb^{III} and As^V as a function of the deposition potential at pH 1, 2 and 3). To decrease the detection limit, the deposition time was increased to 10 min. It was found that the peak height for Sb^{III} was improved by application of a desorption step (−1.2 V for 1 s) at regular intervals (every 2 min) during the deposition step. The peak intensity of 2 nM Sb^{III} increased by 30% if a desorption step was applied half way through a 4 min deposition step. Using a deposition potential of −0.18 V, a deposition time of 10 min and application of a 1 s desorption at −1.2 V every 2 min, the detection limit was determined in an acidified seawater (50 mM HCl) spiked with 100 pM Sb^{III}. The relative standard deviation for 9 consecutive measurements was 14% giving a LOD of 42 pM (~5 ppt) which is comparable to the LOD obtained using a Hg film electrode [48] and more recently on a bismuth film [45]. The stability of the signal obtained at such low levels also demonstrate that the conditions used in this work (20 μM hydrazine, 50 mM HCl) do not cause a reduction of Sb^V, which is present at levels 50–100 times higher (~1 to 2 nM) in the seawater. Typical SC scans obtained at low levels of Sb^{III} (<1 nM) are shown in Fig. 5. Although low, these detection limits were still too high for commonly encountered Sb^{III} levels in Liverpool Bay waters (≤0.1 nM Sb^{III}).

3.3. Optimum conditions for the determination of As^{III}

The deposition potential experiment (Fig. 3) shows that Sb^{III} is deposited at all deposition potentials where As^{III} is accumulated.

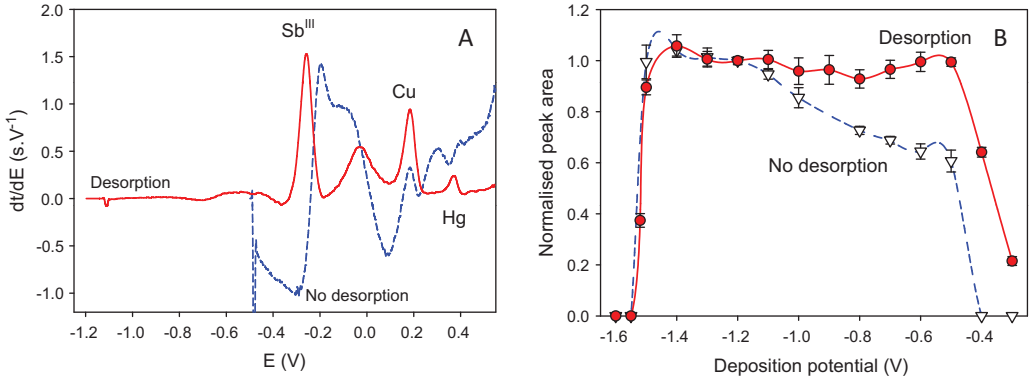

Fig. 4. Effect of the desorption step (−1.2 for 2 s) on 5 nM (A) and 10 nM (B) Sb^{III} peak in deaerated sea water, pH 8.4. (A) Subtracted scans with and without desorption. (B) Effect of varying the deposition potential with and without desorption.

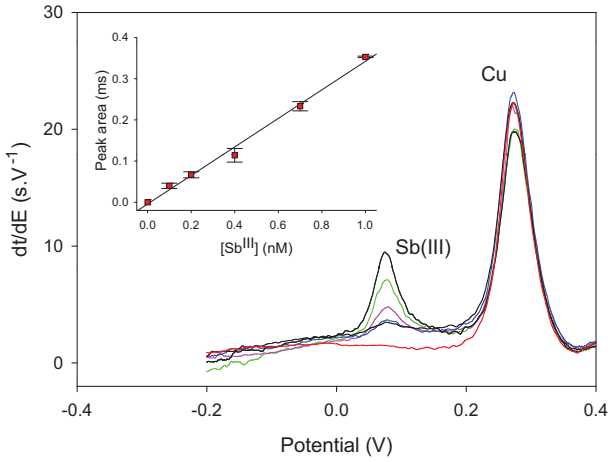

Fig. 5. Examples of typical subtracted ASC scans in acidified seawater (50 mM HCl) with low levels of Sb^{III} (0, 0.1, 0.2, 0.4, 0.7 and 1 nM); analytical scans [E_{dep} = −0.18 V (120 s), E_{des} = −1.2 V (1 s)] repeated 5 times, 1 s eq, stripping from −1.2 V to 0.55 V, i_{ox} = 4 nA; background scans: 0.55 V (10 s), −1.2 V (5 s), 1 s eq, stripping from −1.2 to 0.55 V, i_{ox} = 4 nA.

For this reason, it is useful to determine [Sb^{III}] separately from As^{III} so that correction can be made by subtraction from [As^{III} + Sb^{III}] to find [As^{III}]. At natural pH, the arsenite peak is at ~−0.25 V and de-oxygenation is required for the low levels reported in marine waters (<0.1–4 nM). Also, at natural pH, it was found that the oxidation product (As^{III}, possibly a chloro-hydroxo species) of As^0 briefly adsorbs on the gold electrode; this is described below for selective discrimination against Sb^{III}, making concentration subtraction unnecessary.

3.3.1. *Natural pH with interference from Sb^{III}*

Detection of As^{III} in presence of oxygen was attempted by using fast scan rates (up to 2000 Hz in SWASV and high oxidation current in ASC) but the resulting signals were too noisy or wide. Solutions had to be deoxygenated.

It was recently shown that when Mn^{II} is reduced at the gold electrode during the accumulation step at neutral pH, reduction of arsenate also occurs [30] whose stripping peak is indistinguishable from As^{III} (since it corresponds to the same oxidation reaction, i.e. As^0 to As^{III}). The amount of arsenate deposited was found directly correlated to the amount of Mn^0 removed from the surface, suggesting a reduction of As^V to As^{III} through the oxidation of Mn^0 to Mn^{2+} [30]. The net effect is that, in conditions where Mn^{II} is co-deposited during the deposition step, both As^V and As^{III} give a response but with different sensitivity [30]. In coastal waters, the concentration of Mn^{II} can amount to >100 nM in summer conditions [59], sufficiently to interfere with the determination of As^{III}. To remediate this problem, the deposition of manganese during the deposition step must be prevented. Two methods were found here appropriate: (1) deposition at potentials where Mn^{II} is not co-deposited ($E_{dep} \geq -0.9$ V); (2) addition of EDTA to prevent Mn^{II} deposition through chelation. Testing was done in UV-digested sea water from Liverpool Bay containing 212 ± 12 nM of Mn^{II}. The water was first UV-digested to oxidise all potential As^{III} to As^V. No As signal was observed when depositing at −0.9 V (indicating that all As^{III} had become oxidised to As^V) while the As^V peak was apparent after deposition at −1.2 V, as recently reported [30]. Upon additions of EDTA, the As^V peak decreased until complete disappearance at EDTA > 600 μM (Fig. 6A). Note that the Cu peak is largely unaffected by additions of EDTA because the Cu-EDTA complex is electroactive at this negative deposition potentials [57]. Addition of 5 nM As^{III} showed that EDTA did not interfere with the detection of arsenite. This procedure is similar to that used for reductive groundwaters containing high levels of Mn and Fe [60].

Although As^{III} can be detected by using a deposition potential ≥−0.9 V without addition of EDTA, it was generally found difficult to measure reliably sub-nM levels due to low peak intensity and a variable baseline. In the presence of 600 μM EDTA and using low deposition potentials (≤−1.2 V), the peak was always better shaped and lower detection limits were achieved. This improvement is probably due to less adsorption of dissolved organic matter (DOM) on the gold surface at more negative deposition potential. An example of typical scans obtained by the standard addition methods are shown in Fig. 6B.

3.3.2. *Natural pH without interference from Sb^{III}*

Conditions were optimised to minimise Sb^{III} interference which is co-deposited with As^{III} (Fig. 3). At the end of the deposition step and before the desorption step, the potential was switched for 1 s to an "intermediate potential" (IP) whose value was varied from negative (−0.4 V) to positive values (0.55 V) (Fig. 7A). When IP = −0.4 V, similar signals were obtained for As^{III} and Sb^{III}. When IP was more positive than the stripping potential, both As^0 and Sb^0 were oxidised. However, the As^{III} signal was still relatively high during the stripping step while Sb^{III} signal decreased sharply. This shows that As^{III} remained adsorbed at the gold surface after reoxidation. When IP > +0.2 V, As^{III} signal sharply decreases which may be due to As^V formation. Optimum IP value was chosen at +0.15 V. Although the As^{III} signal is 40% lower than when IP = −0.4 V, the baseline is flatter and the peak is better shaped. The adsorbed species were however not stable as shown by the exponential decrease of As^{III} with IP time (Fig. S4). This might be due to complexation of As^{III} with chloride as such instability was not observed in non-chloride solution (Fig. 2A) or in groundwater [55].

3.3.3. *Acidic conditions*

The method was optimised using a 2-min deposition time at pH 3, 2 and 1 in presence of hydrazine. Typical responses obtained at these pH for As^V, As^{III} and Sb^{III} are shown in Fig. S3. The optimum deposition potential for As^{III} determination is as negative as possible without inducing reduction of As^V, i.e. −0.7 V at pH 2–3 (Fig. S3). Detection limits of As^{III} were determined by repetitive ASC measurements in pH 2 seawater containing 80 μM hydrazine and spiked with 0.5 nM As^{III} using E_{dep} = −0.7 (120 s) and E_{des} = −1.2 V (1 s). The detection limits was 70 pM (RSD = 5.1%) but could be further lowered by increasing the deposition time. In acidic conditions, Sb^{III} interferes with As^{III} determination and must be first determined and subtracted.

3.4. *Determination of combined inorganic iAs (As^{III} + As^V)*

Previous work has shown that iAs in seawater is best detected after acidification to pH 1 [25] or at natural pH after addition of Mn^{II} and HOCl [30]. A problem with the acidic method is that monomethyl arsenic acid MMA, DMA (and to a small extent iSb) can be co-deposited during the stripping step so the voltammetric signal is a combination of these species [25].

By looking at the effect of pH, we found that at pH ≥ 1.6 (E_{dep} = −1 V), addition of 20 nM MMA, 20 nM DMA or 20 nM Sb did not interfere. Although the sensitivity is lower than at pH 1, SWASV can be used at pH 1.6 for determination of iAs. This was tested in NASS-6 and a concentration of 18.1 ± 0.6 nM iAs was found, in agreement with the certified value of 19.1 ± 1.6 nM iAs.

At pH ≤ 2, ASC scans were unstable due to increasing oxidation by chemical oxidants produced at the AE. Typical analytical, background and corrected ASC scans for As^V in pH 2 sea water are shown in Fig. 8. A well shaped As peak was obtained for 20 nM As^V (30 s deposition time). Repeated scans showed a gradual

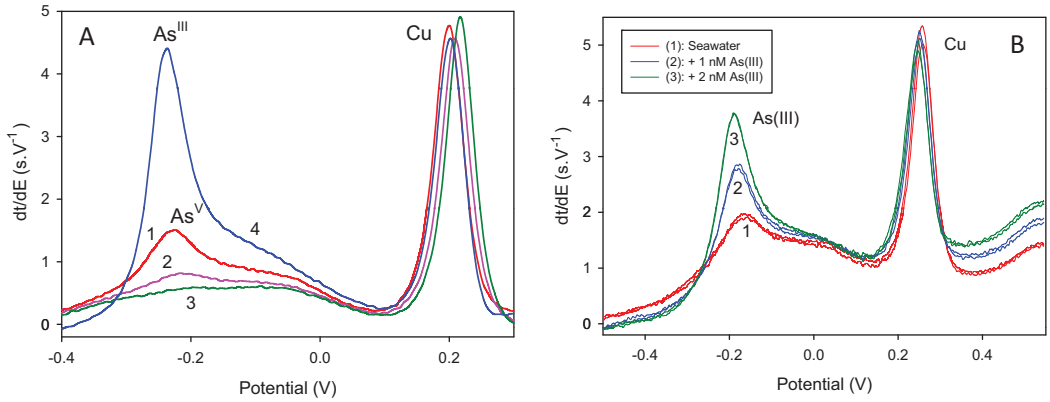

Fig. 6. ASV scans for As^{III} in deoxygenated seawater at pH 8.4 – E_{dep} = −1.2 V; (A) influence of EDTA (1: blank; 2: +200 μM EDTA; 3: +600 μM EDTA; 4: +5 nM As^{III}) (B) Typical calibration curves in a Liverpool Bay sample (Avril 2011, Station 11) determined on-board. (2 measurements per addition and 2 measurements for the blank) – As^{III} additions of 1 and 2 nM.

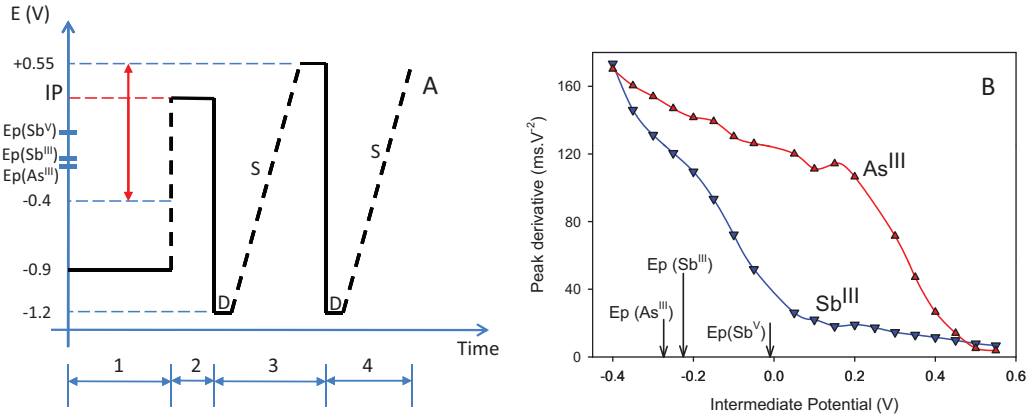

Fig. 7. Procedure to determine As^{III} in the presence of Sb^{III} by selective adsorption during an intermediate potential (IP) step. (A) Schematic representation of the potential variation with time: 1: deposition; 2: IP step; 3: analytical scan; 4: background scan; "D": desorption step, "S": stripping step. (B) Peak derivative for As^{III} and Sb^{III} as a function of the intermediate potential – stripping by ASC. Ep(As^0/As^{III}), Ep(Sb^0/Sb^{III}) and Ep(Sb^{III}/Sb^V) correspond to the relevant peak potentials.

deterioration in the signal which was ascribed to adsorption of dissolved organic matter, as it was eliminated by UV-digestion. To overcome this problem, a cleaning procedure (consisting of −1.5 V for 5 s followed by 5 s at 0.55 V) was applied before each analytical scan. Excellent reproducibility (RSD 2.45%, n = 50) was obtained indicating that the chemical oxidation was negligible at pH 2. This cleaning procedure gave better signals than the application of a desorption potential at −1.5 V. The accuracy of the method was verified using a certified reference material (NASS-6) after fixing the pH to 2 by addition of NH_3. A concentration of 17.0 ± 1.2 nM iAs was found, in agreement with the certified concentration (19.1 ± 1.6 nM iAs). The precision of the method was tested over several days using two different electrodes in NASS-6 and was found very satisfactory (4.3%, n = 6).

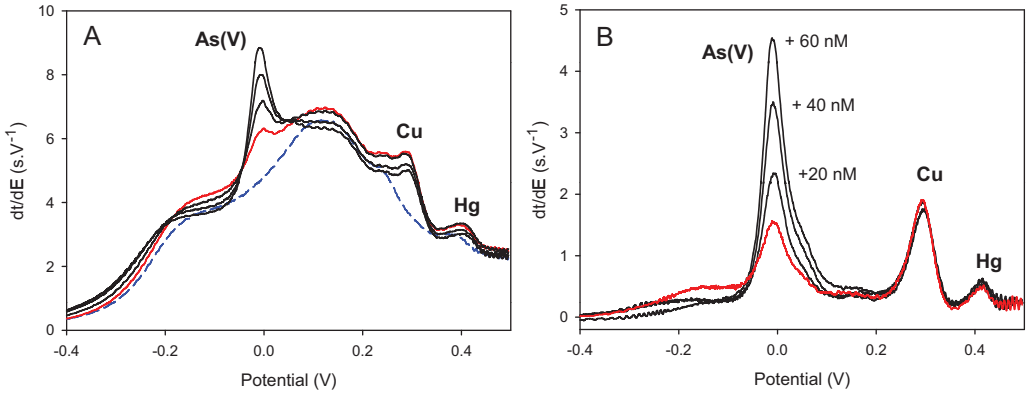

Fig. 8. ASC scans of pH2 sea water. (A) Analytical scans (0.5 V for 5 s, −1 V for 30 s, 1 s equilibrium, i_{ox} = 8 nA up to 0.5 V) with successive additions of 20 nM As(V). The dashed line is the background scan (0.5 V for 5 s, −1 V for 1 s, 1 s equilibrium, i_{ox} = 8 nA up to 0.5 V) of the original signal. (B) Corresponding background-corrected scans (analytical–background). The scans have not been smoothed.

UV-digestion increased the sensitivity by 20–45% and improved the As peak shape (Fig. S5) but same concentrations were obtained with or without UV digestion. Neither MMA nor DMA were found to be destroyed by UV digestion of acidified seawater. In presence of 10 mM persulfate, MMA was converted to As^V but DMA was still resistant to the treatment. In contrast to previously reported observation [25], no peak was observed here for DMA. The reason for this discrepancy is not known.

3.5. Measurement of As^{III}, iAs and iSb in Liverpool Bay coastal waters

As^{III} was determined on-board the RV "Prince Madog" in April 2011 in freshly collected samples from the Irish Sea kept at natural pH and in deoxygenated conditions. Manganese(II) was found to be present so EDTA was added (600 μM) to prevent its interfering effect on the reduction of As^V to As^0 [30] (in order to specifically detect As^{III}). As^{III} was found in all samples (Table 2) with concentrations ranging from 0.44 nM to 1.56 nM (average concentration of 0.9 ± 0.4 nM). Highest concentrations were found close to the coast (shallow depth). The absence of a salinity relationship suggests an input from the sediment, as seen before in estuarine conditions [61,62]. On-board analysis revealed that Sb^{III} levels were below the detection limits. The same samples were analysed 3 weeks later, after storage in the dark at ambient temperature. Still, Sb^{III} levels could not be detected. However, the average As^{III} concentration was much increased during that time (5-fold), reaching up to 8 nM As^{III} indicating that the As speciation is not stable. A similar finding [16] was attributed to high-density polyethylene (HDPE) containers which cannot explain our observations since we used low density (LDPE) bottles.

Table 2
Concentrations of As^{III} in samples from Liverpool Bay (UK). Analysis was done on-board of the RV Prince Madog; samples collected 20–21/04/2011 and analysed within 2 h of collection.

Station no.	Latitude	Longitude	Salinity	Depth (m)	[As(III)] (nM)
13	53°31.998′N	3°30.198′W	33.27	33.8	0.44 ± 0.06
29	53°46.998′N	3°55.398′W	33.75	39.7	0.63 ± 0.03
28	53°46.998′N	3°46.998′W	31.50	38.2	0.61 ± 0.05
22	53°22.998′N	3°38.598′W	32.73	16.0	1.16 ± 0.08
23	53°22.998′N	3°46.998′W	32.75	12.5	1.36 ± 0.10
34	53°22.002′N	3°55.398′W	33.21	20.7	1.56 ± 0.16
33	53°27.000′N	3°55.398′W	33.50	34.1	0.73 ± 0.05
24	53°27.000′N	3°46.998′W	33.20	26.3	0.92 ± 0.09
12	53°27.000′N	3°30.198′W	32.48	15.6	0.78 ± 0.07
11	53°27.000′N	3°21.798′W	32.00	15.9	0.83 ± 0.04

The levels of iSb and iAs in samples collected in Liverpool Bay in June 2009 and March 2010 are shown in Fig. 9. The average concentration for Sb were 0.96 ± 0.45 nM ($n = 13$) and 1.09 ± 0.30 nM ($n = 12$) in June 2009 and September 2010 respectively. The Sb levels show a positive trend with salinity (please note the relatively small range) suggesting an input from the freshwater side. The concentrations of As did not display any relation with salinity in contrast to samples collected in December 2005 [25]. The average concentrations were 15.7 ± 5.5 nM and 13.8 ± 4.5 nM in June 2009 and September 2010 respectively.

Table 3
Summary of stripping methods to be used for inorganic As and/or inorganic Sb speciation in seawater when using a gold electrode. All methods use the background subtraction procedure. *LODs were estimated from experience and correspond to the given deposition time. Highlighted lines correspond to optimum methods for iAs, iSb, As^{III} and Sb^{III} (in acidic and in natural pH conditions) in terms of LODs, interferences and ease of use.

Analyte	Technique	pH	Purging	Conditionning interval Reagent	Edep (V)	tdep (s)	Desorption (V)/ time (s)	Parameters	∅(μm)/ length (μm)	Remarks	Linear range (nM)	LODs SW (nM)	Ref
iAs	SWASV	1	No	None	-1;-1.2	30	No	50Hz, 50 mV, 8 mV	5/200-1000	MMA interferes/small interference from Sb	~0-55	≤ 1*	25
iAs	SWASV	1.6	No	-1.5 V (5s) + 0.5 V (5s)	-1	20-40	No	50Hz, 50 mV, 8 mV	5/ ~220	Automated peak analysis No MMA or Sb^V interference In-situ oxidation of As^{III}	~ 0-50	≤ 2*	This work
iAs	ASC	2	No	-1.5 V (5s) + 0.5 V (5s)	-1	20-40	No	8 nA	5/ ~220	Manual peak analysis No MMA or Sb^V interference In-situ oxidation of As^{III}	~ 0-60	≤ 1 *	This work
iAs	SWASV	8	Yes	+ 1 μM Mn^{II}	-1.3	60	No	50Hz, 50 mV, 8 mV	10/ ~700	Addition of Mn^{II} is required	~ 0-120	2.3	30
As^{III}	SWASV	2	No	+ 20 μM N_2H_4	-0.7	120	-1.2/1s	50Hz, 50 mV, 8 mV	5/ ~220	Hydrazine required to avoid in-situ oxidation Sb^{III} interference	~ 0-10	0.05	This work
As^{III}	ASC	8	Yes	None	-1.2	30	No	3 nA	5/ ~670	Only applicable if no Mn^{II} Need IP if Sb^{III} present	~0-10	0.2	25
As^{III}	ASC	8	Yes	-1.4 V (15s) + 0.5 V (5s)	-0.9	120	-1.2/1s	2 nA	5/ 120	No reagent required Relatively high detection limit - dependent on DOM Need IP if Sb^{III} is present.	~ 0- 10	0.3-1	This work
As^{III}	ASC	8	Yes	+ 600 μM EDTA + IP: 0.15 V (1s)	-1.2	120	No	2 nA	5/ 120	EDTA prevents Mn^{II} effect Need IP if Sb^{III} is present.	~ 0-10	0.07	This work
iSb	DPASV	1	No	None	-1.8	30-120	No	100ms, 4 ms, 50 mV, 6 mV	5/200	No As^V interference Sb^{III} oxidised by chlorine formed at the AE	~ 0-10	≤ 0.1*	44
Sb^{III}	ASC	8	Yes	-1.2 V (15s)+ 0.5 V (5s)	-0.475	300	-1.2/1s	2 nA	5/660	Short E_{dep} range to avoid As^{III} interference	~ 0-10	~ 0.5	This work
Sb^{III}	ASC	1.3	No	+ 80 μM N_2H_4	-0.18	600	-1.2/1s	1.5 nA	5/340	Hydrazine required to avoid Desorption during deposition may help	~ 0-5	0.04	This work

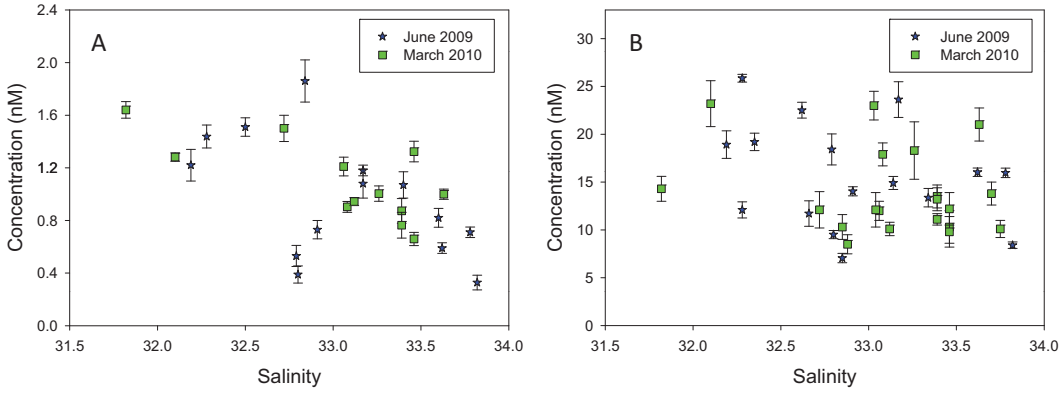

Fig. 9. Concentration of Sb (A) and As (B) as a function of salinity in samples from Liverpool Bay collected in June 2009 (star symbols) and March 2010 (square symbols). Samples acidified to pH 2 and UV digested.

4. Conclusions

Methods for determination of inorganic As and Sb were thoroughly tested at a gold vibrated electrode. The main findings of this work are: (1) iAs is best determined at pH ≥ 1.6 to avoid interferences from MMA or iSb; (2) the marked improvement of the Sb^{III} peak when using a desorption potential; such procedure should be used all the time when using a positive deposition potential; (3) addition of 600 μM EDTA was found optimum to allow sensitive detection of As^{III} while preventing Mn^{II} interference; (4) the reoxidation of As^{III} at the gold surface proceeds through an adsorbed species, allowing the discrimination between Sb^{III} and As^{III} by implementing the intermediate potential procedure; (5) detection limits achieved for Sb^{III} without interference from As^{III} are the lowest reported in seawater at a gold electrode and compare favourably with detection limits obtained at Hg electrodes; (6) UV digestion improves the sensitivity but no systematic increase in iAs nor iSb were observed, suggesting partial blockage of the electrode surface.

The methods summarised in Table 3 were developed in both acidic conditions and natural pH. They might give ground to further speciation studies to look at e.g. complexation or adsorption of these metalloids. These methods were tested and optimised using coastal waters from Liverpool Bay.

Acknowledgements

Carmel Pinnington (Liverpool University, School of Environmental Sciences) made the SEM images. The crew of RV "Prince Madog" is gratefully acknowledged for assistance with sampling. P.S. benefits from an EPSRC fellowship (EP/E061303) and acknowledges the Life Science Interface (LSI) programme for financial support. GA acknowledges a grant scholarship (SFRH/BD/46521/2008). The authors acknowledge the anonymous reviewers for their helpful comments in improving the quality of the manuscript.

Appendix A. Supplementary data

Supplementary data associated with this article can be found, in the online version, at http://dx.doi.org/10.1016/j.aca.2012.08.013.

References

[1] M.O. Andreae, Deep-Sea Res. 25 (1978) 391–402.
[2] P.J. Statham, J.D. Burton, W.A. Maher, Deep-Sea Res. 34 (1987) 1353–1359.
[3] M. Filella, N. Belzile, Y.W. Chen, Earth-Sci. Rev. 57 (2002) 125–176.
[4] G. Howard, S.W.D. Comber, Appl. Organomet. Chem. 3 (1989) 509–514.
[5] P. Anninou, R.R. Cave, Estuar. Coast. Shelf Sci. 82 (2009) 515–524.
[6] G.A. Cutter, L.S. Cutter, Geochem. Geophys. Geosyst. 7 (2006).
[7] G.A. Cutter, L.S. Cutter, Mar. Chem. 49 (1995) 295–306.
[8] G.A. Cutter, L.S. Cutter, Mar. Chem. 61 (1998) 25–36.
[9] G.A. Cutter, L.S. Cutter, A.M. Featherstone, S.E. Lohrenz, Deep-Sea Res. Pt II 48 (2001) 2895–2915.
[10] F.L. Hellweger, K.J. Farley, U. Lall, D.M. Di Toro, Limnol. Oceanogr. 48 (2003) 2275–2288.
[11] A.R. Kumar, P. Riyazuddin, Int. J. Environ. Anal. Chem. 87 (2007) 469–500.
[12] J.Y. Cabon, N. Cabon, Anal. Chim. Acta 418 (2000) 19–31.
[13] J.Y. Cabon, N. Cabon, Fresen. J. Anal. Chem. 368 (2000) 484–489.
[14] J.Y. Cabon, C.L. Madec, Anal. Chim. Acta 504 (2004) 209–215.
[15] A. D'Ulivo, I. Paolicchi, M. Onor, R. Zamboni, L. Lampugnani, Spectrochim. Acta B 64 (2009) 48–55.
[16] R.E. Rivas, I. Lopez-Garcia, M. Hernandez-Cordoba, Spectrochim. Acta B 64 (2009) 329–333.
[17] J.M. Serafimovska, S. Arpadjan, T. Stafilov, Microchem. J. 99 (2011) 46–50.
[18] L. Zhang, Y. Morita, A. Sakuragawa, A. Isozaki, Talanta 72 (2007) 723–729.
[19] B. Staniszewski, P. Freimann, Spectrochim. Acta B 63 (2008) 1333–1337.
[20] J.E. Portmann, J.P. Riley, Anal. Chim. Acta 35 (1966) 35.
[21] Q. Zhang, H. Minami, S. Inoue, I. Atsuya, Anal. Chim. Acta 508 (2004) 99–105.
[22] P. Michel, B. Boutier, A. Herbland, B. Averty, L.F. Artigas, D. Auger, E. Chartier, Oceanol. Acta 21 (1998) 325–333.
[23] A.M. Featherstone, E.C.V. Butler, B.V. O'Grady, P. Michel, J. Anal. Atom. Spectrom. 13 (1998) 1355–1360.
[24] G.A. Cutter, Deep-Sea Res. 38 (1991) S825–S843.
[25] P. Salaün, B. Planer-Friedrich, C.M.G. van den Berg, Anal. Chim. Acta 585 (2007) 312–322.
[26] H.L. Huang, D. Jagner, L. Renman, Anal. Chim. Acta 207 (1988) 37–46.
[27] J. Vandenhecke, M. Waeles, R.D. Riso, P. Le Corre, Anal. Bioanal. Chem. 388 (2007) 929–937.
[28] G. Dugo, L. La Pera, V. Lo Turco, G. Di Bella, Chemosphere 61 (2005) 1093–1101.
[29] Y.C. Sun, J. Mierzwa, M.H. Yang, Talanta 44 (1997) 1379–1387.
[30] K. Gibbon-Walsh, P. Salaün, C.M.G. van den Berg, Anal. Chim. Acta 710 (2012) 50–57.
[31] L. La Pera, G. Di Bella, R. Rando, L.T. Vincenzo, G. Dugo, Environ. Monit. Assess. 145 (2008) 119–126.
[32] J. Zima, C.M.G. Vandenberg, Anal. Chim. Acta 289 (1994) 291–298.
[33] A. Profumo, D. Merli, M. Pesavento, Anal. Chim. Acta 539 (2005) 245–250.
[34] L. Jiajie, Y. Nagaosa, Anal. Chim. Acta 593 (2007) 1–6.
[35] J. Long, Y. Nagaosa, Int. J. Environ. Anal. Chem. 88 (2008) 51–60.
[36] F. Quentel, M. Filella, Anal. Chim. Acta 452 (2002) 237–244.
[37] G. Gillain, G. Duyckaerts, A. Disteche, Anal. Chim. Acta 106 (1979) 23–37.
[38] C. Brihaye, G. Gillain, G. Duyckaerts, Anal. Chim. Acta 148 (1983) 51–57.
[39] G. Gillain, C. Brihaye, Oceanol. Acta 8 (1985) 231–235.
[40] C.M.G. Vandenberg, S.H. Khan, P.J. Daly, J.P. Riley, D.R. Turner, Estuar. Coast. Shelf Sci. 33 (1991) 309–322.
[41] G. Capodaglio, C.M.G. Vandenberg, G. Scarponi, J. Electroanal. Chem. 235 (1987) 275–286.
[42] O.D. Renedo, M.J.A. Martinez, Anal. Chim. Acta 589 (2007) 255–260.
[43] O.D. Renedo, M.J.A. Martinez, Electrochem. Commun. 9 (2007) 820–826.
[44] P. Salaün, K. Gibbon-Walsh, C.M.G. van den Berg, Anal. Chem. 83 (2011) 3848–3856.
[45] P. Zong, Y. Nagaosa, Microchim. Acta 166 (2009) 139–144.
[46] A. Mardegan, P. Scopece, F. Lamberti, M. Meneghetti, L.M. Moretto, P. Ugo, Electroanalysis 24 (2012) 798–806.
[47] L. Chen, N. Zhou, J. Li, Z. Chen, C. Liao, J. Chen, Analyst 136 (2011) 4526–4532.
[48] V. Tanguy, M. Waeles, J. Vandenhecke, R.D. Riso, Talanta 81 (2010) 614–620.
[49] C.S. Chapman, C.M.G. van den Berg, Electroanalysis 19 (2007) 1347–1355.
[50] Z. Bi, C.S. Chapman, P. Salaün, C.M.G. van den Berg, Electroanalysis 22 (2010) 2897–2907.

[51] P. Salaün, C.M.G. van den Berg, Anal. Chem. 78 (2006) 5052–5060.
[52] C.E. Banks, A.O. Simm, R. Bowler, K. Dawes, R.G. Compton, Anal. Chem. 77 (2005) 1928–1930.
[53] H.L. Huang, D. Jagner, L. Renman, Anal. Chim. Acta 202 (1987) 123–129.
[54] I.M. Kolthoff, R.L. Probst, Anal. Chem. 21 (1949) 753–754.
[55] K. Gibbon-Walsh, P. Salaün, C.M.G. van den Berg, Anal. Chim. Acta 662 (2010) 1–8.
[56] F. Quentel, M. Filella, C. Elleouet, C.L. Madec, Sci. Total Environ. 355 (2006) 259–263.
[57] K. Gibbon-Walsh, P. Salaun, C.M.G. van den Berg, J. Phys. Chem. A 116 (2012) 6609–6620.
[58] Y. Louis, P. Cmuk, D. Omanovic, C. Garnier, V. Lenoble, S. Mounier, I. Pizeta, Anal. Chim. Acta 606 (2008) 37–44.
[59] K. Gibbon-Walsh, P. Salaün, C. Van den Berg, Environ. Chem. 8 (2011) 475–484.
[60] K. Gibbon-Walsh, P. Salauen, M.K. Uroic, J. Feldmann, J.M. McArthur, C.M.G. van den Berg, Talanta 85 (2011) 1404–1411.
[61] J. Vandenhecke, M. Waeles, J.-Y. Cabon, C. Garnier, R.D. Riso, Estuar. Coast. Shelf Sci. 90 (2010) 221–230.
[62] M. Waeles, J. Vandenhecke, P. Salaün, J.-Y. Cabon, R.D. Riso, J. Mar. Syst. (2011), http://dx.doi.org/10.1016/j.jmarsys.2011.09.008.